CHIMIA 40 (1986) Nr. 1 (Januar)

Potential of Surface Enhanced Raman Scattering for Catalytic Research

Alexander Wokaun* and Alfons Baiker*

Present investigations of catalytic reaction mechanisms increase the demand for direct spectroscopic observation of the molecular processes occuring at the catalyst surface. Interdisciplinary research is essential to advance our knowledge in this field. We have therefore decided to explore the application of surface enhanced Raman scattering (SERS) for the in situ characterization of solid state catalysts. The fascinating phenomenon of surface enhancement is outlined in this article. The high sensitivity achieved is used to study amination reactions of aliphatic alcohols on copper catalysts. Results from surface enhanced Raman spectroscopy provide information on the mechanism which complements the evidence obtained from chemical and kinetic investigations. Enhanced Raman spectra of adsorbates have been recorded on the surface of a technical copper catalyst under reaction conditions. The design of this substrate has been guided by combining the conditions for strong surface enhancement with the requirements for a catalyst that is stable at elevated temperatures in the presence of surface active adsorbents. The scope of SERS as a novel surface analytical tool in catalysis is evaluated, and an outlook to envisaged applications is given.

1. Introduction

Surface characterization techniques[1] have an enormous impact on the understanding of chemical reactions occurring at surfaces and interfaces. Recently a novel phenomenon has attracted strong interest of research groups involved in surface studies due to its potential for surface analytics. A variety of optical processes have been found to be strongly *enhanced* on suitably roughened metallic surfaces[2]. The stimulus for research in this field was the observation of giant enhancements in the Raman scattering intensity from pyridine adsorbed on roughened Ag electrodes by *Fleischmann* et al.[3]. Careful quantitative measurements by *Jeanmaire* and *Van Duyne*[4] established that this high signal intensity was not caused by an increase in surface area, but that the Raman scattering cross section *per molecule* was enhanced by factors on the order of 10^6.

* *Correspondence:* Privatdozent Dr. A. Wokaun
Laboratorium für Physikalische Chemie
and
Privatdozent Dr. A. Baiker
Technisch-chemisches Laboratorium
Eidgenössische Technische Hochschule Zürich
ETH-Zentrum, Universitätstrasse 22 and 6
CH-8092 Zürich

Intensive research efforts towards elucidation of the origins of the enhancement have established the importance of two classes of mechanisms. The *electromagnetic contribution* is based on the presence of amplified local fields close to a metallic surface. All electromagnetic processes at the surface can be enhanced by this phenomenon[2, 5]. For the analytical applications of surface Raman scattering, it is important to note that the Raman intensities will be enhanced for *any* adsorbed species within the range of the amplified local fields, which typically extend out to a distance corresponding to several adsorbed monolayers. Requirements for electromagnetic enhancement are a specifically prepared surface morphology, which exhibits roughness in a defined size range, and suitable dielectric properties of the metal. This is the reason why most investigations have been carried out on group «IB» metal substrates (Cu, Ag, and Au). This mechanism, which contributes factors of 10^3–10^4 to the enhancement of Ag, will be outlined in Section 2.

A second contribution to the enhancement originates from the «*chemical*» interactions of the adsorbate with the metal[6]. It has been shown that light-induced charge transfer processes play an important role in this mechanism. The requirement for molecular donor or acceptor levels involved in the charge transfer explains why this enhancement contribution has predominantly been observed with aromatic molecules[6]. Special surface sites (adatom clusters) are important for the charge transfer as they facilitate the light-induced creation of electron–hole pairs[7]. The chemical mechanism may contribute enhancement factors on the order of 10^2–10^3 on cold-deposited metal films; it is, however, molecule specific.

To cover the entire range of possible applications of the enhancement phenom-

Alexander Wokaun: Geboren am 19. Oktober 1952 in Darmstadt. Studium der Chemie an der Eidgenössischen Technischen Hochschule (ETH) Zürich 1970–74; Promotion 1978. Forschungsaufenthalte am IBM Research Laboratory in San Jose, California (1979–80), und an den Bell Laboratories in Holmdel, New Jersey (1980–81). Seit 1982 Leiter einer Forschungsgruppe auf dem Gebiet der Oberflächenspektroskopie am Laboratorium für Physikalische Chemie der ETHZ. 1983 Habilitation für das Lehrgebiet Physikalische Chemie.

Alfons Baiker: Geboren am 14. April 1945 in Zürich. Studium der Chemie an der Eidgenössischen Technischen Hochschule (ETH) Zürich 1967–71; Promotion 1974. Wissenschaftlicher Mitarbeiter und später Oberassistent am Technisch-chemischen Laboratorium (TCL) der ETHZ 1974–77. 1976 Austauschstipendiat im «International Younger Research Worker Interscheme», Aufenthalt am Imperial und University College London. 1978–79 Forschungs- und Lehrtätigkeit an der Stanford University, California. 1980 Habilitation für das Lehrgebiet Katalyse an der ETHZ. Seit 1980 Leiter einer Forschungsgruppe auf dem Gebiet der Heterogenen Katalyse am TCL-ETHZ.

enon is outside the scope of this article. A variety of linear and nonlinear optical processes have been investigated. Some of the envisaged applications include surface enhanced photochemistry[8–10], and dynamic processes at surfaces occurring under laser excitation[11, 12]. Considerable attention has been devoted to laser assisted adsorption and desorption processes[13], and to chemical transformations in photocatalytic reactions[14, 15]. Other surface processing techniques which can possibly benefit from the enhancement phenomenon include laser annealing[11, 16] and microfabrication processes such as lithography[17], photodeposition[11, 12, 18], and photoetching[19]. A more comprehensive survey has been given elsewhere[20].

Here we would like to focus on the potential of surface enhanced Raman scattering (SERS) in catalytic research. A joint research project, carried out at the Physical Chemistry Laboratory and the Department of Industrial and Engineering Chemistry of ETH Zurich, has been devoted towards developing SERS into a surface analytical tool which can be applied to study catalyst surfaces during reaction. Recent progress will be illustrated in Section 3, using the adsorptive interaction of amines with copper catalyst surfaces as a case study. The information obtained on this system by enhanced Raman spectroscopy complements the evidence gained by a variety of methods applied in catalytic research. In the concluding Section 4, an outlook to anticipated trends and future developments of the field will be presented.

2. Electromagnetic Enhancement Mechanism

Electromagnetic processes close to a surface can be enhanced by the presence of local fields $\boldsymbol{E}_{loc}$ that are *amplified* by a local field factor $L(\omega)$[2, 5, 21] as compared to the incident laser field $\boldsymbol{E}_0$,

$$\boldsymbol{E}_{loc} = L(\omega)\,\boldsymbol{E}_0 \qquad (1)$$

For Raman scattering by an adsorbate, the enhancement factor EF of the Raman intensity relative to the free molecule can be written in the form[2, 5]

$$EF = |L(\omega_{laser})\,L(\omega_{Raman})|^2 \qquad (2)$$

Equation (2) reflects the fact that both the incident laser field, of frequency ω_{laser}, and the Raman light emitted at $\omega_{Raman} = \omega_{laser} - \omega_{vib}$, are potentially enhanced by the presence of the surface. In numerical evaluations of Eq. (2) the geometries of excitation and detection, and a proper average over adsorbate positions on the surface must be taken into account. An important consequence of the nonlinearity of the Raman scattering phenomenon is seen from Eq. (2): If the surface supports a local field enhancement $L(\omega)$ on the order of 10 at both relevant frequencies, the Raman scattering cross section will be enhanced by $EF \approx 10^4$, which is the electromagnetic enhancement contribution mentioned in Section 1.

Here we would like to present a simple model how such a field enhancement can arise on a particle surface. A single spheroidal metal particle of dimensions small compared to one wavelength, which corresponds to the Rayleigh scattering limit, will be considered. A more rigorous treatment that includes the effects of finite particle size and dipolar interactions among the metal particles on the substrate has been presented in detail elsewhere[20–22].

The local field $\boldsymbol{E}_{tip}$ at the surface of a prolate spheroid, shown schematically in Fig. 1, is determined from the relation

$$\boldsymbol{E}_{tip} = L_z(\omega)\,\boldsymbol{E}_0 = \frac{\varepsilon(\omega)}{1 + [\varepsilon(\omega) - 1]\,A_z}\,\boldsymbol{E}_0 \qquad (3)$$

where $\boldsymbol{E}_0$ is the incident field of frequency ω, directed along the major axis z of the spheroid, and $\varepsilon(\omega)$ is the complex, frequency dependent dielectric constant of the material. In the Rayleigh limit A_z is a constant that depends solely on the geometry of the spheroid; it is bounded to the range $0 \leqslant A_z \leqslant 1$, and is termed a «depolarization constant»[23, 24].

The local field factor $L_z(\omega)$ given by Eq. (3) contains two contributions:

(1) the concentration of the electromagnetic field at points of high curvature on the surface, known as the «lightning rod effect»[24], and
(2) the local field enhancement due to surface plasma oscillations.

The latter effect is illustrated in Fig. 1. The applied field $\boldsymbol{E}_0$ creates a surface charge distribution that oscillates at the frequency ω. The amplitude of the surface charge oscillation, and thereby the local field enhancement, are maximum if ω coincides with the eigenfrequency of the system, which corresponds to resonant excitation of a localized surface plasmon[2, 5]. The resonance condition is easily derived from Eq. (3): the maximum of $|L(\omega)|^2$ occurs when the real part of the denominator vanishes, i.e. when

$$1 + [\mathrm{Re}\{\varepsilon(\omega_{res})\} - 1]A_z = 0 \qquad (4)$$

For a sphere, $A_z = 1/3$, which yields $\mathrm{Re}\{\varepsilon(\omega_{res})\} = -2$. Prolate spheroids polarized along their major axis have $0 \leq A_z \leq 1/3$, and thus $\mathrm{Re}\{\varepsilon(\omega_{res})\}$ takes on more negative values.

The notion of a negative dielectric constant may appear unfamiliar at first. With non-absorbing dielectric substances, such as quartz, $\varepsilon(\omega)$ is real and positive: in such cases $|\boldsymbol{E}_{tip}| < |\boldsymbol{E}_0|$, as is seen from Eq. (3). For metals, however, the presence of free conduction electrons gives rise to a negative real part of the dielectric constant at frequencies below the volume plasma frequency of the material (for a short discussion, cf.[21]). As an example, the function $\mathrm{Re}\{\varepsilon(\omega)\}$ for silver[25] is shown in Fig. 2. This function is negative for wavelengths larger than 330 nm, and exhibits a strong decrease in the red spectral region. The wavelengths of resonant surface plasmon excitation are indicated in Fig. 2 for spheres and prolate spheroids of eccentricities 2:1 and 3:1. A pronounced red shift of the plasmon resonance with increasing eccentricity is clearly seen.

The resonant nature of the electromagnetic enhancement was first verified in the experiments of *Liao* et al.[26]. The authors studied Raman scattering from adsorbed $CN^{\ominus}$ ions on an array of uniformly sized and shaped silver particles, that had been produced using lithographic techniques[26]. A resonance in the excitation energy dependence of the enhancement factor was detected; the variation of the resonance frequency with particle eccentricity was found to follow the behavior predicted from Eq. (4)[26].

Next let us consider the value of the local field enhancement at resonance, which is

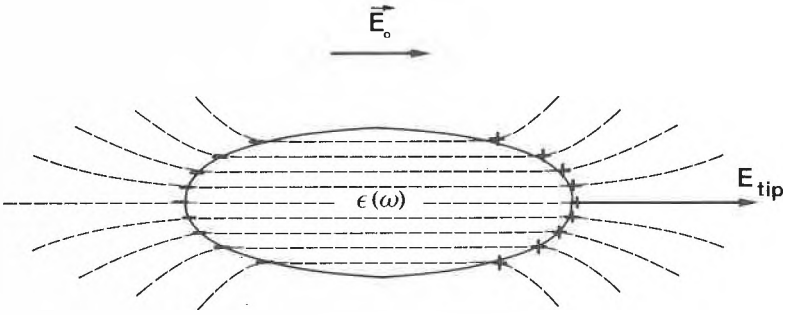

Fig. 1. Local field enhancement near the surface of a spheroidal metal particle. The laser field $\boldsymbol{E}_0$ produces a dipolar surface charge distribution which oscillates with the frequency ω of the electromagnetic wave. The amplitude of the surface charge oscillation is largest if the metal dielectric function $\varepsilon(\omega)$ fulfills the resonance condition, Eq. (4), for surface plasmon excitation. The local field is maximum ($\boldsymbol{E}_{tip}$) at the points of highest curvature, due to the so-called lightning rod effect (see text).

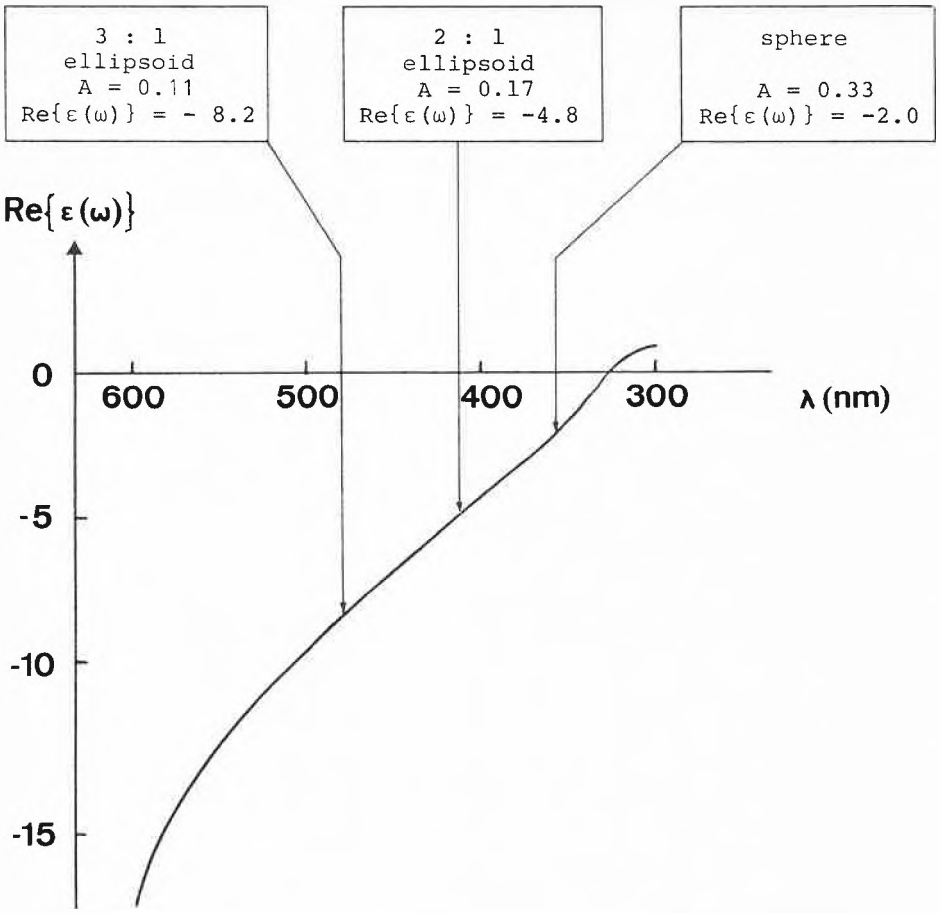

Fig. 2. Surface plasmon resonances for small silver spheroids. The real part of the dielectric function $\varepsilon(\omega)$ for silver [25] is plotted as a function of wavelength. The resonance conditions for spheres and prolate ellipsoids of eccentricities 2:1 and 3:1 are indicated by arrows [cf. Eq. (4)].

determined from Eq. (3),

$$|L_z(\omega)| = \left|\frac{\varepsilon(\omega)}{\mathrm{Im}\{\varepsilon(\omega)\}A_z}\right| \qquad (5)$$

For high local field enhancement, a material with low loss, i.e. small values of $\mathrm{Im}\{\varepsilon(\omega)\}$, is required. One might compare the particle with a resonant cavity: the quality factor and hence the local fields will be high if the losses are low. This requirement explains the exceptional role of the group «IB» elements in surface enhancement. Silver has very low losses throughout the visible spectrum, as evidenced by its uniformly high reflectivity. Copper and gold are good reflectors only for longer wavelengths, and therefore appear reddish to the eye; in the green and blue spectral region these elements are absorbing due to interband transitions. Consequently wavelengths longer than 580 nm must be used to excite enhanced Raman scattering on copper and gold substrates. For silver all visible wavelengths are suitable for excitation as long as the resonance condition, Eq. (4), is fulfilled.

The importance of low losses becomes most evident if we recall that the enhancement is proportional to $|L(\omega)|^4$ according to Eq. (2). Unfortunately, most transition metals exhibit losses $\mathrm{Im}\{\varepsilon(\omega)\}$ that are typically five to ten times higher than those of silver in the visible spectral range. Consequently only much smaller enhancements can be expected on transition metal surfaces.

Hitherto we have considered a particle of dimensions small compared to a wavelength, without further specifying its size. A careful consideration of size-dependent effects [22, 27–29] is, however, essential in determining the relatively narrow range of particle dimensions for which strong Raman enhancements can be observed. If the particle size is too small, the conduction electrons suffer additional losses by collisions with the surface of the particle; thereby the «quality» of the resonator is reduced [27]. If the particle dimensions are larger than $\lambda/10$ radiation damping effects [27] become important: the size of the resonant polarization is reduced as the dipole looses its energy efficiently due to radiation [27]. Simultaneously a red-shift of the plasmon resonance frequency is observed. These effects have first been predicted by *Mie* in a classical calculation [28] of the scattering by colloidal metallic spheres.

An exact numerical calculation for prolate silver spheroids of 2:1 eccentricity has been carried out by *Barber* et al. [29]. Results of a self-consistent calculation [22] are illustrated in Fig. 3 where the enhancement $|E_R/E_0|^2$ of the radial surface field E_R, relative to the exciting laser field E_0, is plotted as a function of wavelength. The radius a of the silver sphere is the second parameter. With increasing radius, the enhancement curve is broadened and the maximum is strongly decreased due to radiation damping. The red shift of the enhancement maximum with increasing

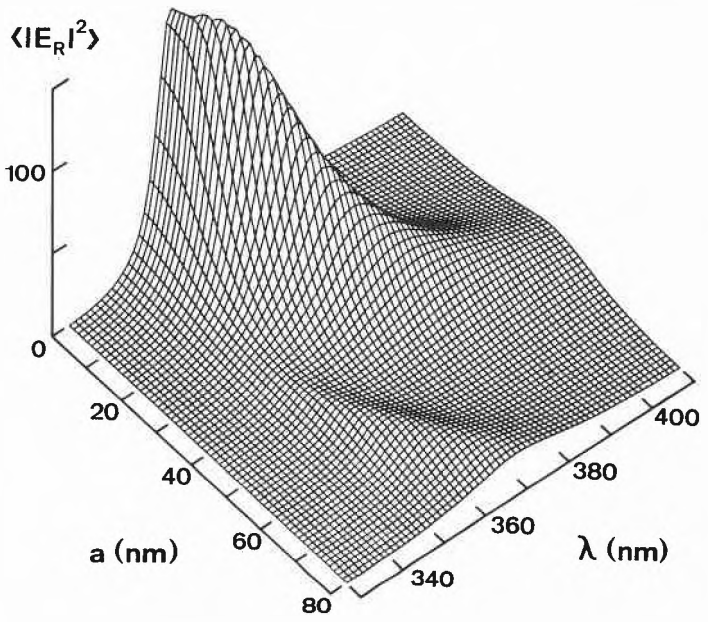

Fig. 3. Size dependence of the surface enhancement. The surface-averaged local field enhancement $|E_R/E_0|^2$ for spheres is plotted as a function of wavelength λ [22]. With increasing radius a, the dipolar surface plasmon resonance is broadened, decreased in magnitude by radiation damping, and red-shifted due to dynamic depolarization [22]. The second enhancement maximum visible at short wavelengths ($\lambda \approx 360$ nm) for the larger spheres is due to the quadrupolar surface plasmon.

size due to «dynamic depolarization»[22] is also apparent in Fig. 3. For the larger radii a second enhancement maximum is visible, which is due to excitation of the quadrupolar surface plasmon[22].

For maximum surface enhancement, particles must be large enough to avoid losses due to electronic surface collisions, and small enough to avoid eccessive radiation damping[27]. A detailed evaluation[30] has shown that the optimum radius for a silver sphere is 20 nm; for prolate silver spheroids of eccentricities 2:1 and 3:1 the enhancement is maximum for long half axis dimensions of 30 nm and 35 nm, respectively. For copper particles, optimum half axis dimensions that are somewhat larger (60–80 nm) have been calculated[30].

To conclude this section we remark that interactions among the metal particles on the surface must be taken into account for a quantitative modelling of the surface enhancement. This is outside the scope of this article, and the reader is referred to recent publications for a theoretical discussion[20, 21] and experimental verification[31] of dipolar interaction effects.

In the following section we shall focus on the application of the enhancement phenomenon in catalysis. A case study of *N*-alkylation reactions on Cu catalysts will be used as an example.

3. Case Study: *N*-Alkylation Reactions on Copper Catalysts

Studies on the mechanism of catalytic routes for the synthesis of aliphatic amines are important in view of their large-scale industrial applications. The amines constitute intermediates in the synthesis of fabric softeners, emulsion stabilizers, pigment dispersers, and agricultural products. Several drugs, herbicides, pesticides, dyes, and other chemicals contain amino groups which originate from reactions with such intermediates. The application of higher aliphatic amines and their derivatives, as e.g. quarternary ammonium compounds, is mainly based on their cationic surface activity. Changes in surface and colloidal properties can be achieved by small quantities of such substances. The products from *N*-alkylation reactions have found applications in almost every field of modern technology and agriculture[32].

Among several methods which have been proposed for the synthesis of aliphatic amines[33], catalytic amination of alcohols has gained increasing importance in recent years. It represents an economic way particularly for the synthesis of long-chain aliphatic amines. A variety of supported metal catalysts have been proposed to be suitable for catalytic amination. For a series of catalysts activities and selectivities have been compared in our laboratory under identical conditions[34, 35]. As a test reaction we have used the amination of dodecanol with mono- and di-methylamine to produce *N*-methyl- and *N*,*N*-dimethyl-dodecylamine, respectively; e.g.

$$CH_3(CH_2)_{11}-OH + HN(CH_3)_2 \xrightarrow[cat]{H_2} CH_3(CH_2)_{11}-N(CH_3)_2 + H_2O \quad (6)$$

This study revealed that copper supported on γ-Al_2O_3 is most effective for amination.

3.1. Reaction Mechanism

A general reaction pathway has been proposed[36] which is shown in Fig. 4 for the case of monomethylamine reactant. It is based on GC-MS analysis of the products obtained under various reaction conditions, kinetic measurements, and isotope labeling experiments. Essential steps are the dehydrogenation (I) of the alcohol, condensation (II) of an adsorbed aldehyde-type species with adsorbed methylamine, release of water (III), and hydrogenation (IV) of the resulting enamine-type species. This pathway is confirmed by the observation of aldehyde and enamine side products which are not necessarily reaction intermediates, but may be equilibrated with surface intermediates of related structure (cf. Fig. 4). The dehydrogenation of the alcohol (step I) is catalyzed by copper. Steps II and III can occur unassisted by a catalyst[37]. The hydrogenation of the enamine-type intermediate (step IV) is again catalyzed by the metal. The necessity of catalyst participation in step IV is confirmed by the work of *Kliger* et al.[38] on the hydroamination of ketones and aldehydes. A thermodynamic consideration of the reaction pathway indicated that equilibria are favourable for reaction steps III and IV; these reactions constitute the driving force for the overall reaction. The α-amino-alcohol is not observed due to its very low equilibrium concentration.

Reactions performed with α,α-dideuterated alcohols exhibited a significant kinetic isotope effect. The mixture of the amination products contained no dideuterated product amines. Undeuterated and monodeuterated products were found in a ratio of 1.9. The absence of dideuterated product amines indicated the abstraction of an α-hydrogen, and is consistent with the formation of an aldehyde-type species as a reaction intermediate. The hydrogen abstraction is non-equilibrated, as evidenced by the small (6–10%) isotopic exchange of the reactant alcohol. This supports the idea that abstraction of an α-hydrogen atom represents the rate-determining step of the overall process.

Kinetics were investigated in the absence

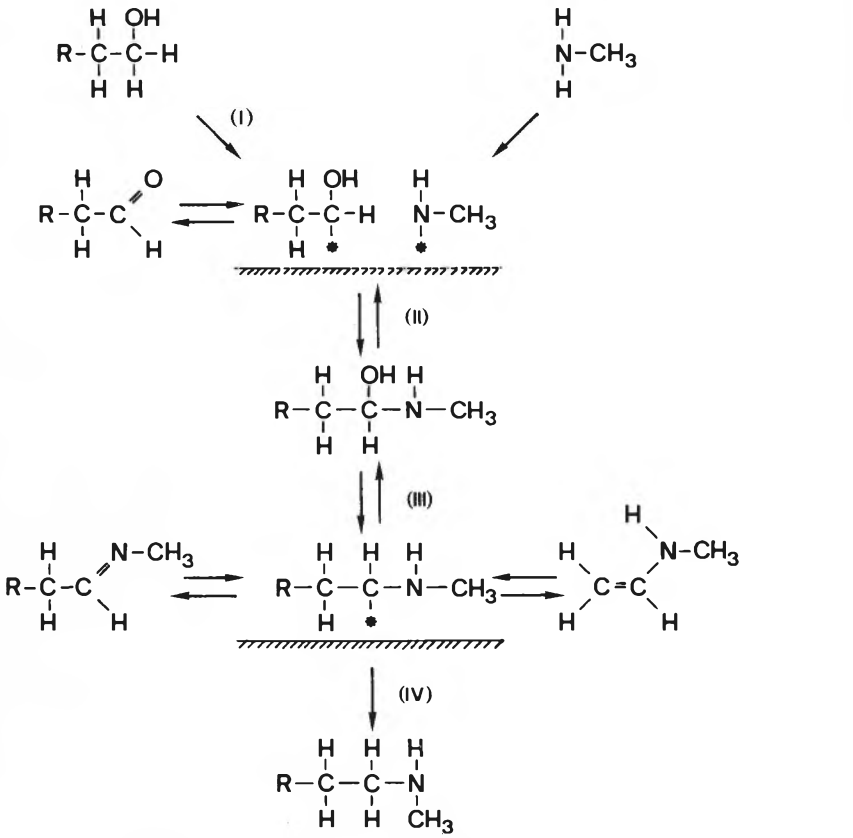

Fig. 4. Pathway of N-alkylation reactions on Cu catalysts[36]. *The reactant alcohol is dehydrogenated (step I) to form an aldehyde-type species* $RCH_2CH(OH)-*$, *where the asterisk denotes a surface site. Subsequent steps are the formation of an α-amino-alcohol (II), release of water (III), and hydrogenation (IV) of the enamine-type species* $RCH_2CH(*)-NHCH_3$ *to form the product amine. Equilibrated side products that have been detected in the product stream are the aldehyde* (RCH_2CHO) *and the enamine/imine tautomer pair.*

of mass transfer limitations for the amination of octanol with dimethylamine in both the gas and liquid phases. Gas phase kinetics could be described by the rate equation

$$r = k_0 \frac{K_{ROH}\, p_{ROH}}{(1 + \sum_i K_i\, p_i)^2} \qquad (7)$$

where K_i and p_i are the adsorption equilibrium constants and partial pressures of species i, respectively. The assumptions implied in this rate equation are: (i) the rate determining step of the overall reaction involves the abstraction of an α-hydrogen atom, and its transfer to an adjacent vacant site; (ii) single site Langmuir adsorption for the reactants and products. Assumption (i) is justified by the results of the isotope labeling experiments. Inhibition of the reaction was found to be significant (at the 95% confidence limit) for octanol, water, and dimethylamine, whereas no significant inhibition by hydrogen was found in the partial pressure range 1–40 kPa. The observed activation energy of 65 ± 5 kJ/mol is compatible with abstraction of an α-hydrogen from an alcohol as the rate determining step. The activation energy depends only weakly on the chain length of the aliphatic alcohols; it is independent of the amination agent and of the support for low dispersions of copper.

The foregoing discussion illustrates that the interaction of reactant and product amines plays an important role in the reaction mechanism. These interactions are also very important in connection with possible deactivation processes, as will be discussed in Section 3.4.

3.2. *Adsorption of m-Toluidine*

Toluidine was chosen as a species which contains two functionalities of interest. The interactions of both the amino group and the aromatic π-electron system with the copper surface can be investigated.

SERS experiments have been designed to decide between the two principal bonding models presented in Fig. 5. Dissociative bonding involves the breaking of an N–H bond and formation of a covalent bond between nitrogen and the metal. Lithium *m*-toluidide was selected as a model compound resembling this bonding type. Associative bonding is accompanied by partial charge transfer from the nitrogen lone pair to the copper conduction band. The protonated toluidinium ion, in which the nitrogen lone pair interacts with the charge of the proton, corresponds to this second bonding type. Our strategy was to compare the SERS spectrum of *m*-toluidine adsorbed on Cu with the Raman spectra of the two model compounds, and the spectrum of neat *m*-toluidine liquid.

For SERS experiments the Cu substrates have to fulfill the requirements on surface morphology discussed in Section 2. Metal catalysts are usually used as powders or in high dispersion on a support. First experiments on Cu powders are reported below in Section 3.3. For the toluidine studies we have used a model catalyst surface that was produced starting from Cu foils. Major advantages are the better control of the surface morphology, good thermal conductivity, and the simple geometry which is very suitable for the surface Raman experiment. These advantages are achieved at the expense of lower thermal stability and a considerably smaller surface area, as compared to copper powder and supported Cu systems.

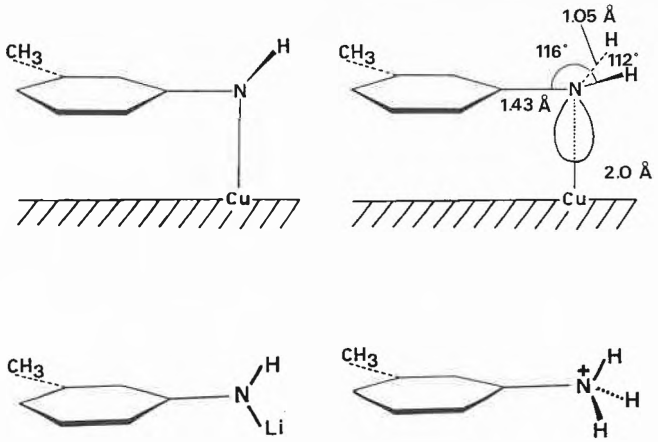

Fig. 5. Bonding of m-toluidine to the copper surface. Lithium m-toluidide is a model compound for dissociative bonding (left); the toluidinium ion resembles an associative bonding situation (right) where the molecule is bound to the surface via the nitrogen lone pair.

Two preparation procedures have been tested to create the required surface roughness on Cu foils: chemical etching in 2M HNO_3 solution at room temperature, and a combination of sandblasting and etching. Surface morphologies obtained by using these procedures are shown in the scanning electron micrographs presented in Fig. 6. If one starts from an unpretreated Cu foil (Fig. 6a), the etching process is relatively slow. Highest surface Raman enhancements were achieved for etching times of 30 min, which result in the sponge-type surface presented in Fig. 6b. It is seen that this surface exhibits abundant roughness on the 10–100 nm scale which produces the strongest local field enhancements (cf. Section 2). Pretreatment by sandblasting enlarges the Cu foil surface area markedly (Fig. 6c) by exposing crystal grain boundaries, but the dimensions of the created roughness (≈ 1 μm) are too large to result in electromagnetic enhancement. However, sandblasting accelerates the subsequent etching process by an order of magnitude. With 1–3 min of etching the surface enhancement reaches a maximum which is comparable to the one obtained with 30 min of etching only. Note that the combined use of sandblasting and short etching (Fig. 6d) leads to a larger surface area and to morphologies resembling more closely those of classical supported catalysts.

m-Toluidine has been adsorbed on the substrates optimized with respect to surface enhancement (Fig. 6b and 6d). The surface enhanced Raman spectrum is shown in the second trace of Fig. 7. Pronounced differences are seen in comparison with the spectrum of neat *m*-toluidine liquid (third trace). Large frequency shifts occur in the group of bands around 1600 cm^{-1} which correspond to skeletal motions of the aniline ring system. The highest frequency band, which occurs at 1618 cm^{-1} in the free molecule, is up-shifted on Cu. The appearance of a band at 1517 cm^{-1} hints to an interaction of the π-electron system with copper which softens the ring breathing motion. Of central importance for the subsequent argument is the observation of a bond at 1254 cm^{-1} on Cu, which is absent in the spectrum of the neat liquid. The torsional motions around 520 cm^{-1} merge into a broad band on the surface, indicative of an inhomogeneous distribution for the hindered motions of the molecule on the surface.

The similarity between the spectra of toluidine adsorbed on Cu and of the toluidinium ion suggests that the toluidine molecule is bound to the copper surface by the nitrogen lone pair. The associative bonding model was confirmed by a partial normal coordinate analysis [39]. The geometry corresponding to a good fit between experimental and calculated spectra is indicated in Fig. 5. The value found for the Cu–N bond length, 2.0 Å, is typical for copper–amine complexes in solution. The calculated vibrational frequencies reflect the shifts observed, and account for the observed additional vibration band at 1254 cm^{-1}. Indications of the interaction of the π-electron system with the copper surface are seen in the SERS spectrum (1517 cm^{-1} and 1578 cm^{-1} bands), but have not been evaluated in more detail. In conclusion, the comparison of the model compound spectra with the SERS spectrum (second trace in Fig. 7) and the normal coordinate analysis indicate that for room temperature adsorption, *m*-toluidine binds to the surface via the nitrogen lone pair, without N–H bond dissociation.

With regard to the higher temperatures used in the catalytic reaction, it will be important to monitor possible changes in

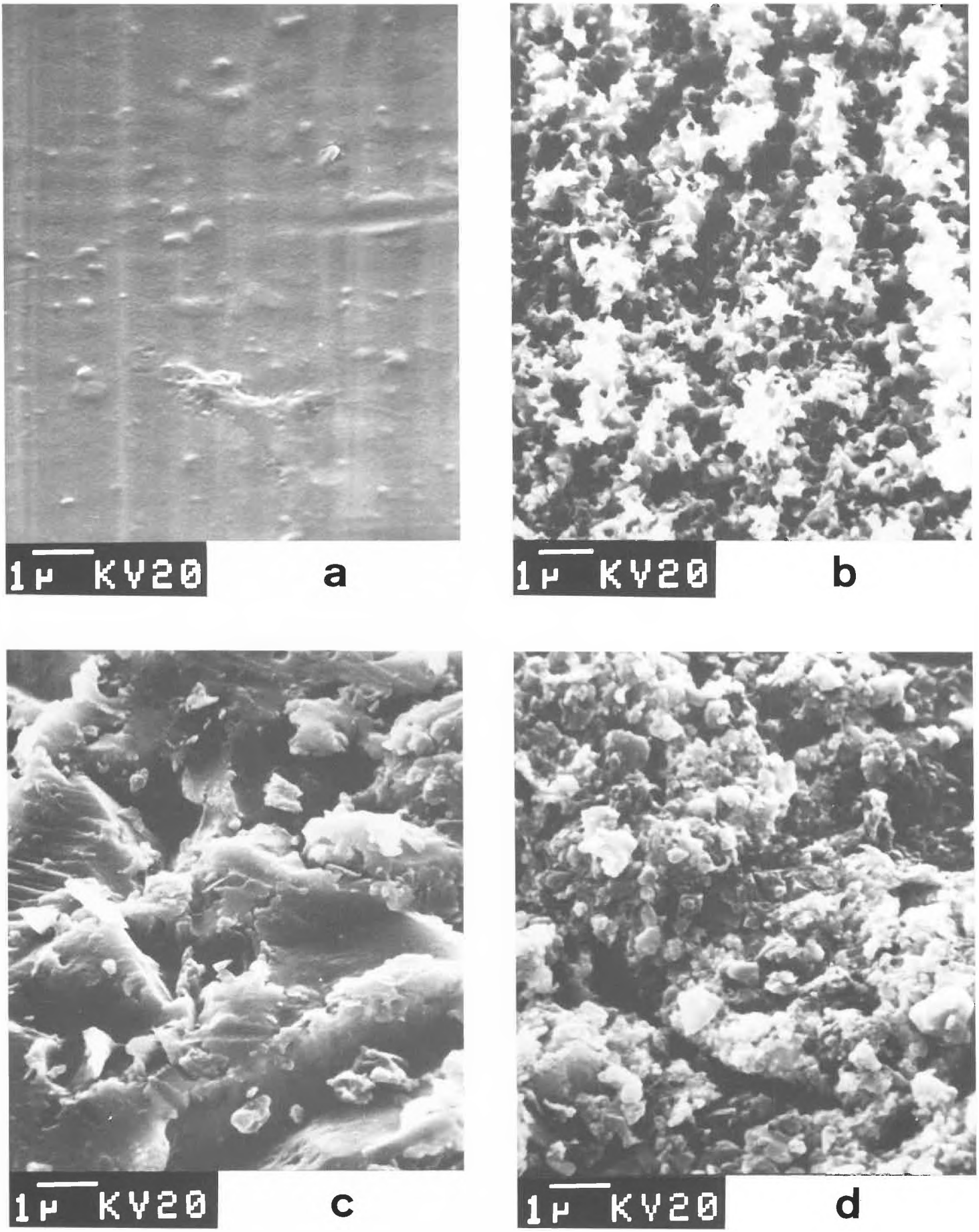

Fig. 6. Surface morphology of copper substrates for surface enhanced Raman scattering. Two roughening procedures have been developed [40] *starting from commercial 0.1 mm copper foil (a). A 30 min room temperature etch in 2M HNO_3 creates the sponge-type surface shown in (b) which gives rise to high surface enhancement. Alternatively the copper foil is preroughened by sandblasting with 600 grain Al_2O_3 (c) and then subjected to a short (2 min) etch to create abundant roughness in the 10–100 nm size range (d) which is optimum for surface enhancement.*

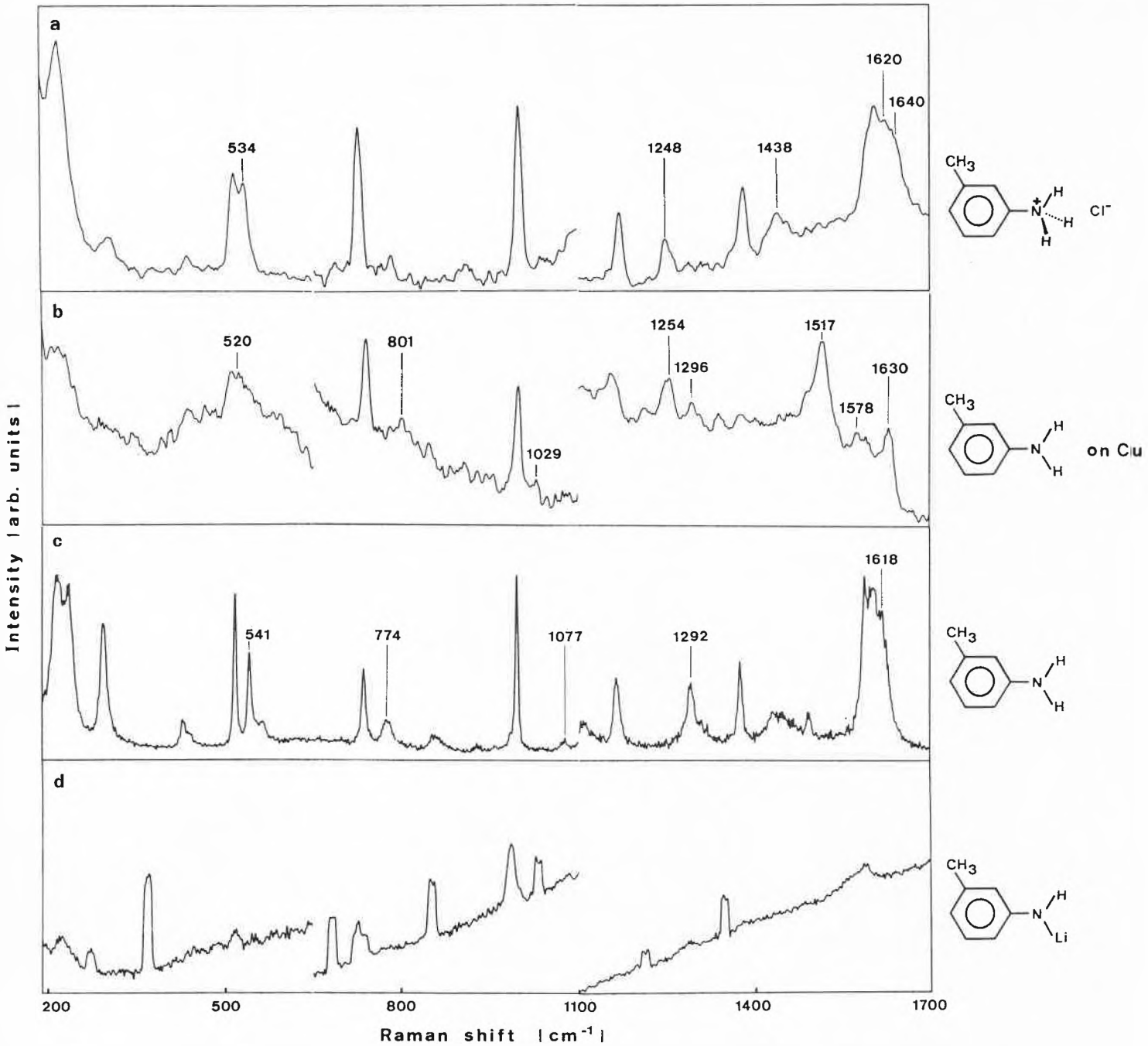

Fig. 7. Raman spectra of adsorbed m-toluidine and model compounds. The surface enhanced Raman spectrum from adsorbed molecular layers of m-toluidine on copper (trace b) exhibits significant changes as compared to the spectrum of the neat liquid (trace c). Raman spectra of the model compounds [m-toluidinium ion in solution (trace a) and lithium m-toluidide (trace d)] are included for comparison.

the bonding with temperature. Extensions of the measurement to reaction temperatures (150–200 °C) are presently being performed.

From the amine adsorption we proceed to the investigation of catalytic amination reactions, shown in the reaction mechanism of Fig. 4. The complexity of the spectra resulting from the co-adsorption of two reactants can be circumvented by selecting an intramolecular variant of the above reaction. A good candidate is the production of piperidine from 5-amino-pentanol.

3.3. Cycloaminations

It has recently been shown[41] that supported copper exhibits high activity and excellent selectivity not only for the bimolecular reaction, but also for the corresponding intramolecular cyclization. Besides the cyclization of 5-amino-pentanol, cycloamination of 4-amino-butanol to pyrrolidine, and of 2-(*o*-aminophenyl)-ethanol to indole have been performed with selectivities higher than 90%. These reactions, as they start from only one reactant, are excellently suited for the investigation of the *N*-alkylation mechanism by surface enhanced Raman spectroscopy.

Very recently we have succeeded[42] to record SERS spectra of molecules adsorbed on a copper powder catalyst, prepared by standard procedures used in catalysis[43]. The Cu powder consists of particles with mean dimensions of 20–30 nm, as determined by X-ray diffraction line broadening measurements, and was found to show comparable activities and selectivities as the Al_2O_3-supported Cu catalysts.

Spectra of the piperidine product adsorbed on the copper powder catalyst are shown in Fig. 8. On adsorption at 25 °C, only weak signals are detected. Upon raising the temperature to 100 °C, a broad band centered around 1100 cm^{-1} appears. Discrete molecular bands are observed in the top spectrum where the temperature was 150 °C. Several characteristic molecular vibrations are discernible. These preliminary experiments indicate the problems resulting from the low signal/noise ratio observed with Cu powder, which is partly a consequence of the long wave-

length ($\geqslant$ 580 nm) required[40] for excitation. To interpret these spectra, it is of crucial importance to make use of reference spectra which identify the relevant bands.

For this purpose the same molecules have been adsorbed to Ag island films[42]. As compared to copper, silver particles result in a larger enhancement. Spectra can be excited in the green spectral region where the sensitivity of the detection system is maximum. As a consequence surface Raman spectra on the Ag island films can be obtained with excellent sensitivity.

In Fig. 9 the SERS spectrum of piperidine adsorbed on Ag islands is compared with the spectrum of the neat liquid. The SERS spectrum supports the general validity of the associative binding model that was previously derived for *m*-toluidine. This is clearly indicated by the appearance of a (down-shifted) N–H stretch at 3220 cm^{-1} on the surface. More detailed information on the conformation of the adsorbed molecule is obtained by the following observations. The 2730 cm^{-1} and 2803 cm^{-1} C–H stretching modes seen in the neat liquid spectrum are absent in the SERS spectrum. In the free molecule, these lowest-frequency C–H stretches are attributed[44] to the pair of C–H bonds in *trans*-position to the nitrogen lone pair. The absence of these vibrations in the spectrum of the adsorbed molecule can be explained by the reduction of lone pair electron density due to charge transfer in the associative bond, and/or by a preferential conformation of the adsorbed species in which the lone pair is equatorial. Support for this conformation comes from the observation of the very strongly enhanced N–C stretches observed at 992 cm^{-1} and 1158 cm^{-1}. The N–C bonds are closest to the surface and, as the corresponding vibrational dipole has a component perpendicular to the surface, they experience the strongest enhancement.

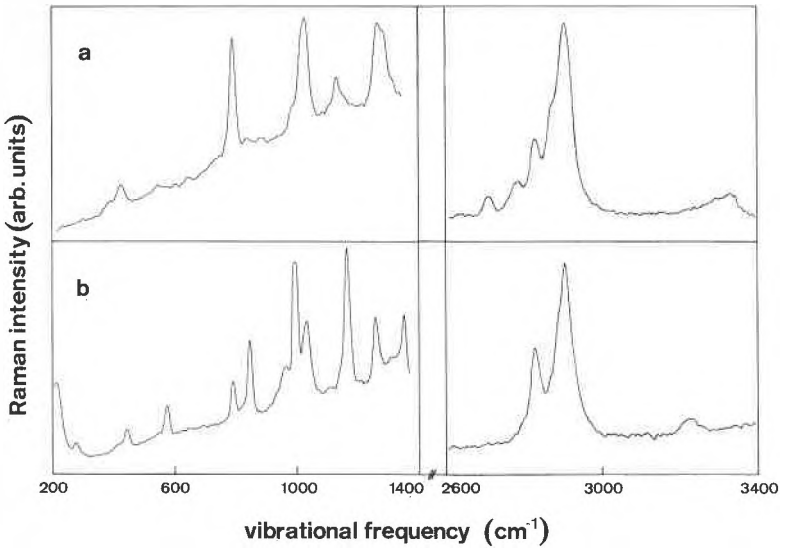

Fig. 9. Surface enhanced Raman spectrum (trace b) of piperidine adsorbed on a silver island film. Prominent changes as compared to the spectrum of the neat liquid (trace a) are the exceptionally strong surface enhancement of the N–C stretches at 992 cm^{-1} and 1158 cm^{-1}, and the missing of the 2730 cm^{-1} and 2803 cm^{-1} C–H stretching vibrations (see text).

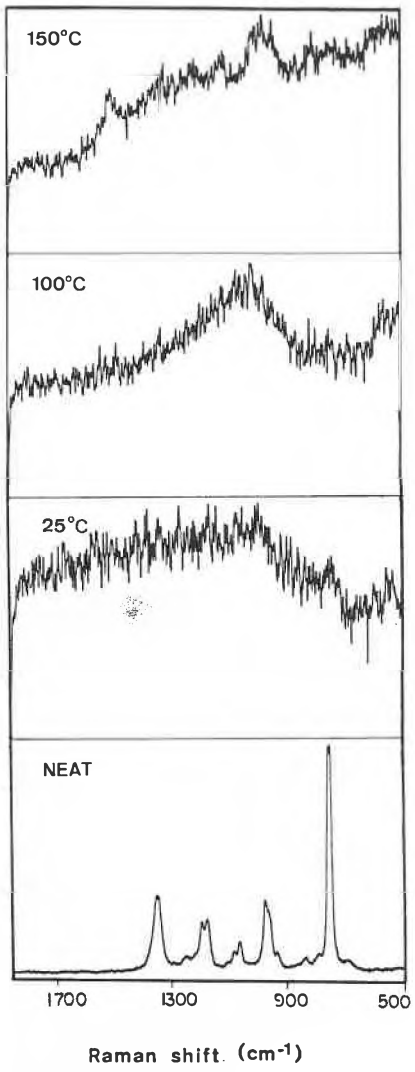

Fig. 8. Adsorption of piperidine on a copper powder catalyst. Surface enhanced Raman spectra have been observed at 25 °C, 100 °C, and 150 °C. The spectrum of neat piperidine liquid is shown for comparison in the bottom trace.

Search for a weakening of the N–C bonds upon adsorption of the amine on copper is of particular interest in view of catalyst deactivation by incorporation of nitrogen into the copper lattice, for which N–C bond breaking is a necessary precursor step.

3.4. Deactivation Caused by Interaction of Amines with Copper Catalyst Surfaces

In general catalytic amination reactions are performed in the presence of hydrogen. It has been shown that in the absence of hydrogen a rapid catalyst deactivation occurs[45]. Fig. 10 illustrates this deactivation

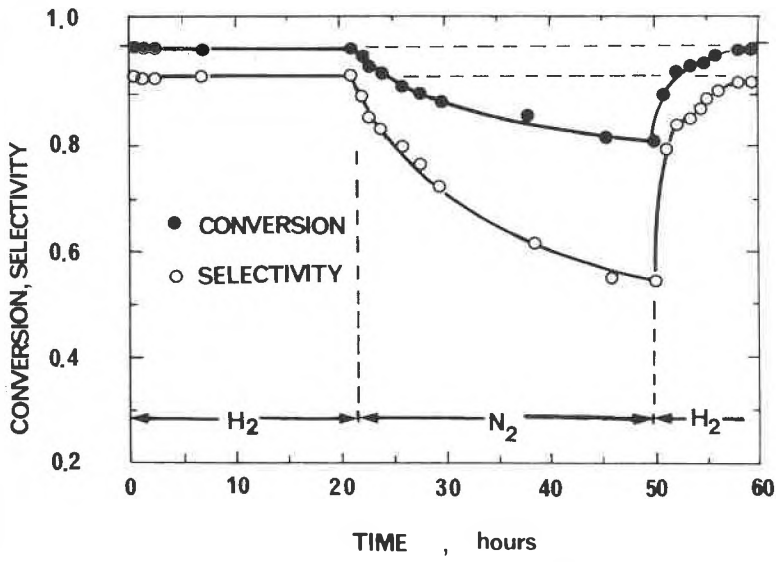

Fig. 10. Influence of hydrogen on the activity and selectivity (to tertiary amine) of the Cu/Al_2O_3 catalyst. The N-alkylation of dimethylamine with dodecanol is investigated in a fixed-bed reactor[45]. When hydrogen in the feed stream is replaced by nitrogen, a rapid catalyst deactivation is observed, which can be reversed by reintroduction of hydrogen.

behavior for the reaction of *n*-dodecanol with dimethylamine. Note the reversibility of the deactivation process upon reintroduction of hydrogen into the system. A similar deactivation is also observed, in the absence of alcohols, during disproportionation of amines on the Cu surface. Temperature programmed desorption (TPD) and differential scanning calorimetry (DSC) studies of deactivated catalysts indicated that the deactivation is caused by incorporation of nitrogen, which originates from the breaking of the N–C and N–H bonds of the corresponding amines. Severe deactivation leads eventually to a Cu_3N surface layer, as has been confirmed by X-ray diffraction[46].

Based on our studies (TPD, TPR, DSC, and SERS) a schematic representation of possible fragmentation processes occurring upon adsorption of amines on a copper surface can be given (Fig. 11). On Cu the primary adsorption step is binding of the nitrogen to the copper, which may be followed by the desired condensation (amination) reaction. Atoms bound directly to the surface are designated by an asterisk; the symbol does not, however, imply any particular number of surface atoms involved in the bonding site. The second step is the formation of a bond between the carbon and an adjacent surface site. C–N bond rupture is followed by incorporation of nitrogen into the metal lattice, or by disproportionation reactions[47]. The structure of the intermediates involved in these processes are not known yet. Hydrogen reduces the surface nitride, forming NH_3, and thereby prevents catalyst deactivation.

In addition to the surface nitride formation which is the deactivation process occuring on Cu, carbon incorporation has been found to be important with metallic Ni and Co catalysts.

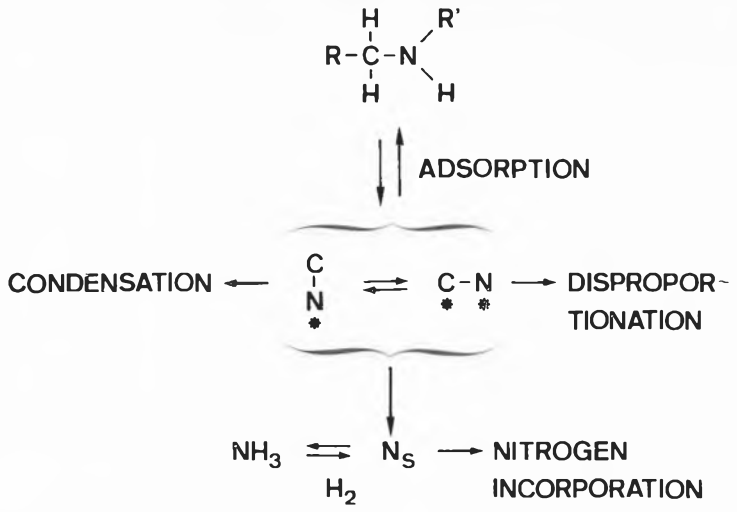

Fig. 11. Interactions of amines with copper surfaces. The adsorbed surface species (see text) can undergo condensation reactions (cf. Fig. 4), disproportionation reactions, or C–N bond cleavage with subsequent incorporation of nitrogen into the Cu lattice. The latter mechanism leads finally to catalyst deactivation by formation of a Cu_3N surface layer. Deactivation can be suppressed by hydrogen due to the reaction $Cu_3N + 3/2\ H_2 \rightarrow 3\ Cu + NH_3$.

4. Outlook

The fascinating phenomenon of surface enhancement has provided us with a new technique for the investigation of catalytically active surfaces. Here we have illustrated the potential of this method in a case study of amine interactions with copper surfaces. A crucial step is the preparation of catalytically active surfaces which produce strong electromagnetic enhancement of the Raman scattering cross section for a variety of adsorbates. Present understanding of the size dependence of the enhancement[22, 27–30], and of the influence of particle dipole interactions[20, 21, 31], has resulted in the development of two substrate preparation procedures. Evaporation onto quartz substrates which have been patterned using regular periodic[26, 48] or stochastic[49] masks yields surfaces of group «IB» metal particles which exhibit the highest known enhancements. Experiments on these model surfaces have established the electromagnetic contribution to the enhancement mechanism. While the fabrication of the master quartz substrates is a relatively demanding process, polymer reproduction procedures allow one to produce inexpensive replicas that are compatible with the demands of availability and easy handling necessary for general analytical application.

A disadvantage of the polymer replicas is their lack of stability at temperatures higher than ≈ 150 °C. In this respect the substrates prepared by etching and sandblasting of copper foils offer significant advantages. The energy deposited by laser excitation is dissipated more rapidly due to the high thermal conductivity of the bulk metal material. Thereby the possibility of thermal decomposition of the adsorbates induced by the laser illumination is reduced. The pretreatment by sandblasting and successive etching results in a surface morphology which bears strong similarities with typical porous catalyst surfaces. Electron micrographs show the presence of a broad range of pore sizes, and an abundance of particle-type protrusions in the 10–100 nm size range which contributes most to the observed enhancement.

The most significant advance made towards application of SERS to technical catalysts is the observation of adsorbate Raman spectra on metal powder samples. For the first time we have succeeded to record spectra of amines and alcohols on Cu powder particles, of 20–30 nm mean diameter, which have been prepared by the standard catalyst preparation sequence of precipitation, calcination, and reduction. Information on bonding and geometry of adsorbed molecules has been obtained, which excellently complements evidence on the mechanism gained by chemical and kinetic studies, thermoanalytical methods, and techniques[1] which elucidate structure and chemical composition of the surface.

Attractive routes for further investigations are emerging from this study. Metal particles supported on oxidic carriers (e.g. Al_2O_3 and SiO_2) are presently being investigated in our laboratory. As compared to copper powder they exhibit smaller and well-separated metal particles. Low metal loadings, which generally result in smaller particle sizes, pose high demands on detection sensitivity due to lower electromagnetic enhancement. Supported metal catalysts with relatively high metal loads, such as the ones used in amination reactions, are most promising in this respect.

While the highest enhancements have been observed on the group «IB» metal (Cu, Ag, and Au) preliminary accounts of small enhancements observed on transition metals[50, 51] encourage our efforts to extend SERS investigations to this most important class of catalyst materials. The literature also reports indications[52, 53] for the feasibility of SERS observation on selected alloys. This may open the way for the application of SERS to the wide field of bimetallic and multimetallic catalysts.

A final comment concerns the interesting question whether the surface sites observed by enhanced Raman spectroscopy are identical to those responsible for catalytic activity. To answer this question we may consider three particle size ranges which can be distinguished based on their significantly different properties for catalysis. Our reference catalyst consists of large metal particle grains. *Structure sensitivity* due to geometrical changes in the surface matrix is expected to occur in the particle size range smaller than 10 nm, where the statistics of the surface atoms and ensembles changes significantly[54].

Electronic property changes are expected to influence surface reaction rates only for very small particles. Catalytic reaction rates can be affected if the spacing of the particle energy levels becomes com-

parable to the thermal energy of the reactant. The band spacing d is inversely proportional to the number N of metal atoms in the particle, and is approximately given by[55]

$$d \approx 4\, E_F/(3N) \qquad (8)$$

where E_F denotes the Fermi energy of the metal. For Cu at room temperature, the criterium $d \approx kT$ yields $N \approx 240$, corresponding to a particle size of 2 nm as an upper limit. Both the geometrical arrangement of the atoms on the surface, and the changes in the electronic properties, can influence the structure of the most abundant reaction intermediate (MARI).

Comparing the particle size range where structure sensitivity is likely to occur ($\leqslant 10$ nm), with the range where the Raman enhancement is maximum (10–100 nm), it is apparent that SERS will provide a spectroscopic image of the interaction of *bulk metal surfaces* with adsorbates. However, if we succeed in lowering the particle size range where enhanced Raman spectra are observable significantly below 10 nm, changes in the detected adsorbate composition reflecting changes in the MARI due to structure sensitivity may become detectable.

Although there is a wide span of potential uses of the enhancement phenomenon[20, 21], the results discussed in this survey show that characterization of catalyst surfaces during reaction is one of the most promising applications of surface enhanced Raman scattering. The future research areas which have been discussed give rise to the hope that surface enhanced spectroscopy will have a major impact on catalytic research.

Acknowledgments: Sincere thanks are due to Keith T. Carron and Werner Fluhr who have made essential contributions in the SERS characterization of catalysts, and to Markus Meier for his experimental and theoretical contributions. The authors would like to thank Richard R. Ernst, Werner Richarz, and Urs P. Wild for their continued encouragement and support of this project. Financial support by the Swiss National Science Foundation and the Branco Weiss Foundation is gratefully acknowledged.

Received: November 25, 1985 [FR 21]

[1] A. Baiker, *Chimia 35* (1981) 408, 440, 485; *Int. Chem. Eng. 25* (1985) 16, 30, 38.
[2] A. Wokaun, *Solid State Phys. 38* (1984) 223.
[3] M. Fleischmann, P.J. Hendra, A.J. McQuillan, *Chem. Phys. Lett. 26* (1974) 163.
[4] D.L. Jeanmaire, R.P. Van Duyne, *J. Electroanal. Chem. 84* (1977) 1.
[5] R.K. Chang, T.E. Furtak (Eds.): *Surface Enhanced Raman Scattering,* Plenum, New York (1982).
[6] A. Otto, in M. Cardona (Ed.): *Light Scattering in Solids,* Vol. *4,* p. 289, Springer, Berlin (1983).
[7] J.I. Gersten, R.L. Birke, J.R. Lombardi, *Phys. Rev. Lett. 43* (1979) 147; E. Burstein, Y.J. Chen, C.Y. Chen, S. Lundqvist, E. Tosatti, *Solid State Commun. 29* (1979) 567.
[8] J.I. Gersten, A. Nitzan, *J. Chem. Phys. 75* (1981) 1139.
[9] A. Wokaun, H.P. Lutz, A.P. King, U.P. Wild, R.R. Ernst, *J. Chem. Phys. 79* (1983) 509.
[10] G.M. Goncher, C.A. Parsons, C.B. Harris, *J. Phys. Chem. 88* (1984) 4200.
[11] D. Bäuerle (Ed.): *Laser Processing and Diagnostics,* Springer, Berlin (1984).
[12] *J. Vac. Sci. Technol. B 3* (1985) No. 5 (Proceedings of the Topical Meeting on the Microphysics of Surfaces, Beams, and Adsorbates, Santa Fe, 1985).
[13] T.J. Chuang, I. Hussla, *Phys. Rev. Lett. 52* (1984) 2045.
[14] M. Graetzel (Ed.): *Energy Resources through Photochemistry and Catalysis,* Academic Press, New York (1983).
[15] E. Borgarello, J. Kiwi, E. Pelizzetti, M. Visca, M. Graetzel, *J. Am. Chem. Soc. 103* (1981) 6324; D. Duonghong, J. Ramsden, M. Graetzel, *ibid. 104* (1982) 2977.
[16] P.M. Fauchet, A.E. Siegman, *Appl. Phys. Lett. 40* (1982) 824; D.J. Ehrlich, S.R.J. Brueck, J.Y. Tsao, *ibid. 41* (1982) 630; F. Keilmann, *Phys. Rev. Lett. 51* (1983) 2097.
[17] *J. Vac. Sci. Technol. B 1* (1983) No. 4 (Proceedings of the International Symposium on Electron, Ion, and Photon Beams, Los Angeles, 1983).
[18] D.J. Ehrlich, J.Y. Tsao, *J. Vac. Sci. Technol. B 1* (1983) 969.
[19] T.J. Chuang, *Surf. Sci. Rep. 3* (1983) 1.
[20] M. Meier, A. Wokaun, P.F. Liao, *J. Opt. Soc. Am. B 2* (1985) 931.
[21] A. Wokaun, *Mol. Phys. 56* (1985) 1.
[22] M. Meier, A. Wokaun, *Opt. Lett. 8* (1983) 581.
[23] E.C. Stoner, *Philos. Mag. 36* (1945) 803.
[24] J.I. Gersten, *J. Chem. Phys. 72* (1980) 5779; P.F. Liao, A. Wokaun, *ibid. 76* (1982) 751.
[25] P.B. Johnson, R.W. Christy, *Phys. Rev. B 6* (1972) 4370.
[26] P.F. Liao, J.G. Bergman, D.S. Chemla, A. Wokaun, J. Melngailis, A.M. Hawryluk, N.P. Economou, *Chem. Phys. Lett. 82* (1981) 355.
[27] A. Wokaun, J.P. Gordon, P.F. Liao, *Phys. Rev. Lett. 48* (1982) 957.
[28] G. Mie, *Ann. Phys. 25* (1908) 377.
[29] P.W. Barber, R.K. Chang, H. Massoudi, *Phys. Rev. Lett. 50* (1983) 997; *Phys. Rev. B 27* (1983) 7251.
[30] E.J. Zeman, G.C. Schatz, in *Proc. Seventh Jerusalem Symp. Quantum Chem. Biochem.*, Reidel, Dordrecht (1984).
[31] K.T. Carron, W. Fluhr, A. Wokaun, H.W. Lehmann, *J. Opt. Soc. Am. B* (1986), in press.
[32] *Kirk-Othmer, Encyclopedia of Chemical Technology, 2nd Ed.,* Vol. *2,* Wiley, New York (1963), p. 116–138; *Ullmanns Encyklopädie der technischen Chemie, 4th Ed.,* Vol. *7,* Verlag Chemie, Weinheim (1974), p. 374–399.
[33] A. Baiker, J. Kijenski, *Catal. Rev. Sci. Eng. 27* (1985) 653.
[34] A. Baiker, W. Richarz, *Ind. Eng. Chem. Prod. Res. Dev. 16* (1977) 261.
[35] A. Baiker, W. Richarz, *Helv. Chim. Acta 61* (1978) 1169.
[36] A. Baiker, W. Caprez, W.L. Holstein, *Ind. Eng. Chem. Prod. Res. Dev. 22* (1983) 323.
[37] *Organikum,* VED Deutscher Verlag der Wissenschaften, Berlin (1977).
[38] G.A. Kliger, L.S. Glebov, R.A. Fridman, L.A. Vytnova, A.N. Bashkirov, *Kinet. Katal. 19* (1978) 615; G.A. Kliger, L.S. Glebov, R.A. Fridman, E.I. Bogolepova, A.N. Bashkirov, *ibid. 19* (1978) 619.
[39] A. Wokaun, A. Baiker, S.K. Miller, W. Fluhr, *J. Phys. Chem. 89* (1985) 1910.
[40] S.K. Miller, A. Baiker, M. Meier, A. Wokaun, *J. Chem. Soc. Faraday Trans. I 80* (1984) 1305.
[41] W. Hammerschmidt, A. Baiker, A. Wokaun, W. Fluhr, *Appl. Catal.*, in press.
[42] W. Fluhr, K.T. Carron, A. Baiker, A. Wokaun, unpublished results.
[43] A. Baiker, D. Monti, *Ber. Bunsenges. Phys. Chem. 87* (1983) 602.
[44] F.R. Dollish, W.G. Fateley, F.F. Bentley: *Characteristic Raman Frequencies of Organic Compounds,* Wiley, New York (1974).
[45] A. Baiker, *Ind. Eng. Chem. Prod. Res. Dev. 20* (1981) 615.
[46] A. Baiker, M. Maciejewski, *J. Chem. Soc. Faraday Trans. I 80* (1984) 2331.
[47] A. Baiker, D. Monti, S.F. Yuan, *J. Catal. 88* (1984) 81.
[48] H.W. Lehmann, R. Widmer, M. Ebnoether, A. Wokaun, M. Meier, S.K. Miller, *J. Vac. Sci. Technol. B 1* (1983) 1207.
[49] M. Meier, A. Wokaun, T. Vo-Dinh, *J. Phys. Chem. 89* (1985) 1843.
[50] W. Krasser, A. Ranade, E. Koglin, *J. Raman Spectrosc. 6* (1977) 209; W. Krasser, H. Ervens, A. Fadini, A.J. Renouprez, *ibid. 9* (1980) 80; W. Krasser, *J. Mol. Struct. 80* (1982) 187.
[51] M. Fleischmann, P.R. Graves, I.R. Hill, J. Robinson, *Chem. Phys. Lett. 95* (1983) 322.
[52] T.E. Furtak, J. Kester, *Phys. Rev. Lett. 45* (1980) 1652; Y. Gao, T. Lopez-Rios, *ibid. 53* (1984) 2583.
[53] R.P. Van Duyne, personal communication.
[54] R. van Hardeveld, F. Hartog, *Surf. Sci. 15* (1969) 189.
[55] R. Kubo, *J. Phys. Soc. Jpn. 17* (1962) 975.